Photographic Study of Solid-Gas Fluidization

LEOPOLDO MASSIMILLA and J. W. WESTWATER
University of Illinois, Urbana, Illinois

Motion pictures at 2,000 frames/sec. were used to measure the movements of individual solid particles and gas bubbles in a fluidized bed. Air was used to fluidize 0.028-in. glass spheres and 200-mesh alumina in a 3.75-in. glass column. Aggregates were very common, and each moved as a unit. Particles and aggregates near the wall showed pronounced alternations of fast and slow movements both upward and downward. Individual particles exhibited spin. Baffles increased the bed density and decreased the particle velocities. Small bubbles rose rapidly with little change in shape. Large cavities were slow and tended to collapse and reform elsewhere.

The advantages of a fluidized bed as compared with a fixed bed are the low pressure drop, ease of transportation of the solid from one piece of equipment to another, and good temperature control because of high internal conductivity of the solid-gas system and the high heat transfer rate at the walls. The main disadvantage is poor homogeneity of the fluid as a result of bypassing.

The homogeneity and heat fluxes are of particular importance in catalytic beds, because these factors affect the extent of the conversion and the selectivity of the reaction when competing reactions exist. Many sources report that bubbles, slugs, and channels in fluidized beds are serious handicaps, but they may sometimes be outweighed by the good thermal properties of a fluidized system, especially if a uniform temperature is required or if large quantities of heat must be added or removed.

All these properties depend on the physical distribution and velocity of the solid particles. Baffles or other mechanical devices can be used to destroy bubbles or slugs, but they limit the movement of the solid particles (*11, 12*). An important problem is how much one can afford to reduce the circulation by baffles without nullifying the desired uniformity of temperature in the bed.

Leopold Massimilla is now at the University of Naples, Naples, Italy.

Fig. 1. Free-bed fluidization of 0.028-in. beads; run 5. Height of view = 5.5 in.

Ideally one wishes to know the entire history of movements of the solids and the fluid in a bed. High-speed photography can be used to study the region near the walls. A start was made by Toomey and Johnstone (*23*), who used a metal column fitted with a window. Recently Todd *et al.* (*22*) applied the technique to a two-dimensional column, thin as compared with its width. The present research stressed the photographic technique. One object was to record the motion of individual particles with a high-speed motion picture camera. This required a size magnification at least one order of magnitude larger than that used by prior workers. A second object was to study bubbling. Both still and motion pictures were desired for this. Baffled and free beds could be studied with equal facility.

EXPERIMENTAL

Fluidization Equipment

The column was a 3.75-in.–I.D. glass cylinder, with the lower end fitted to a conic inlet section ending in a distributor consisting of a set of brass screens, the finest being 200 mesh. To minimize bubble generation at the wall, the diameter of the distributor was made ⅝ in. smaller than the column.

Two solids were fluidized in batches: glass beads of 0.028-in. diameter and fluid cracking catalyst of 120 to 200 mesh. Both solids were spheroidal. In each batch about 5% of the particles were colored to serve as tracers. A thin coat of black spray enamel was put on the glass beads, and a bismuth–manganese oxide thin coating on the alumina.

Baffles, when used, were horizontal screens of metal hardware cloth, separated 1 cm. apart by three spacers of copper tubing. Baffles *A*, *B*, and *C* in this paper refer to screens of ⅜-, ¼-, or ⅛-in. hardware cloth.

The fluid used was air from the laboratory line, which passed through a filter, a pressure regulator, and a flow meter. During run 8 part of the air (about 10%) was injected into the bed through a ¼-in. copper tube. The tube passed from the top of the column, down through the bed, made a 180-deg. turn, and emptied upward through a small piece of 200-mesh screen.

During the entire duration of runs 9 and 10 the column was inclined 10 deg. from the vertical. Although this probably modified the flow pattern somewhat, a desirable result was that some gas bubbles were near the wall and their motion could be followed for much greater distances than would have been possible otherwise.

Photographic Technique

Motion pictures were taken with 16-mm. negative film. A selection (*28*) of the results is available on request. For shots encompassing a field of view 3.5 in. high, a 35-mm. focal length lens set at *f*/4 was used, and the lens-to-object distance was about 21 in. Illumination was provided by four spotlights, each 750 w., off to one side at a 45-deg. angle. Two lights were above the camera elevation, and two were below; all were focused on the same spot. Run 10 with alumina powder was photographed in this manner at 2,000 frames/sec.

The other twelve runs listed in Tables 1 and 2 were photographed as close-ups. For these scenes a 1-in. extension tube was connected to the lens, and the lens-to-object distance was adjusted to about 3 in. The field of view was about 0.3 in. high, which is much smaller than that used by prior workers. Enlargements of single frames of movies of the glass particles taken at about 2,000 frames/sec. with an aperture of *f*/2 have been published (*27*). Figure 7 shows alumina at about the same framing speed and was taken at *f*/4.

Still pictures were taken with a 4- by 5-in. negative film. For shots having a vertical field of about 14 in. a 135-mm. focal-length

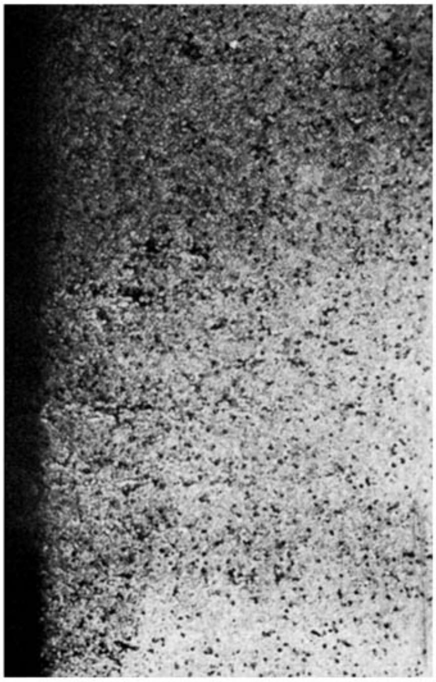

Fig. 2. Baffled-bed fluidization of 0.028-in. beads; run 3. Height of view = 5.5 in.

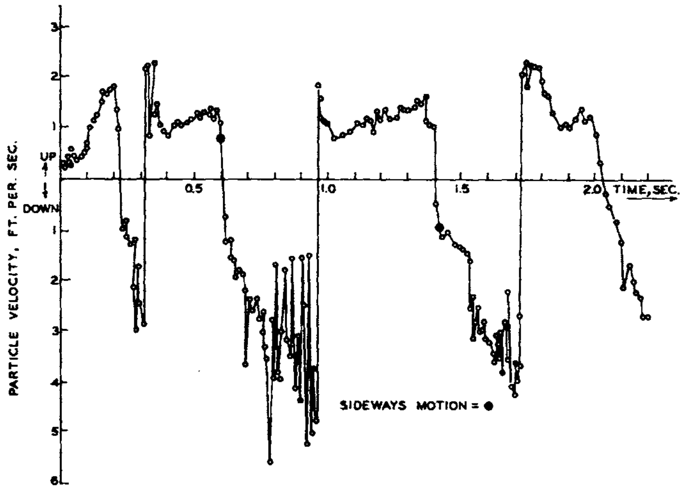

Fig. 3. Velocity of solid particles at the wall. Run 5, 0.028-in. beads, no baffles, superficial air velocity = 2.2 ft./sec.

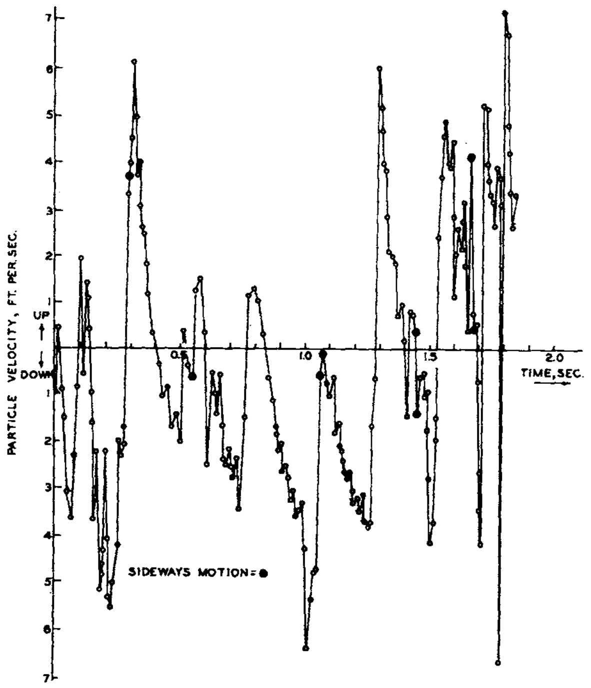

Fig. 4. Effect of gas velocity. Run 4, same as run 5 except that new air velocity = 4.2 ft./sec.

lens located about 21 in. from the column was used. The aperture was $f/4.7$ for the glass beads and $f/5.6$ for alumina, and for each an exposure of 0.001 sec. was used. The illumination was similar to the above except that the spots were spread out to cover 14 in. Figure 8 was taken this way. The column was inclined 10 deg. during the still photograph for Figure 8. The column was vertical during the motion pictures of these same runs (runs 12 and 13).

Close-up still shots were taken from a distance of about 11 in. The resulting field was 5.5 in. high and was illuminated by a flash-tube photolight. Figures 1 and 2 were obtained with an exposure of 1 μ sec. at $f/13$.

The motion pictures were analyzed frame by frame at the screen of a film-editing machine. The screen was fitted with a grid to give readings of the instantaneous space coordinates of individual particles of interest. The instantaneous framing speed of the movie camera was calculated from timing pips on the edge of the film. Thus the displacement of particles from frame to frame was converted to particle velocity in the plane of focus.

The framing rates listed in Tables 1 and 2 are the maximum values which occur at the end of the reels. The value stated in the caption for Figure 7 is the instantaneous speed for the frames selected.

SOLIDS FLOW PATTERN

The particles recorded by the photographic technique are those near the wall. At present no one as devised a successful method for photographing the interior of a fluidized bed. Nevertheless the activity at the wall is worthy of investigation. The velocity of the visible particles frequently changes abruptly in direction and intensity. These sudden changes cause difficulty in measuring and interpreting the data. The observed net flow of solid near the wall is downward, but in the unseen core of the bed the flow must be upward and is stated to be faster than it is near the wall (*2*). The activity of a solid particle depends on its elevation in the bed, with the velocity increasing from the bottom to the top (*23*).

Table 1 lists the characteristics of the systems for which the motions of individual particles were studied photographically, frame by frame. The gross particle motion is summarized in Table 1 as a root-mean-square velocity. The instantaneous velocity at various times is shown in Figures 3 to 6 for four runs. Similar graphs were constructed for the other runs. As a rule the majority of particles visible in a single frame moved in the same direction with the same velocity. Careful measurements were made for a single colored particle until it disappeared. Then a new tagged particle was selected and traced. Thus Figures 3 to 6 show symbols which indicate the successive history of one particle after another.

The most striking features of the graphs are the alternation of fast and slow action and of upward and downward motion. Periodic motion in fluidized beds has been noted previously (*23*).

Glass Particles

For free fluidization the effect of increasing gas velocity is shown in Figures 3 and 4. The amount of solids was not identical in the two runs; however the measurements were taken at the same distance from the top of the bed. An increase in the gas velocity caused an increase in the average velocity of the particles, an increase in the magnitude of the velocity peaks, and an increase in the occurrence of peaks. The peaks show that the particle velocity near the wall is frequently much greater than the calculated superficial gas velocity upward. Most of the peaks are downward velocities, a few are upward, none are sideways. Sideways motion does occur, but it is relatively mild.

The spin of individual particles was observed on occasion. An illustration (*27*) shows an elliptical particle spinning at 105 rev./sec. The spherical particles spin also, but this is more difficult to see. Spin may be important for heat and mass transport; however it has not been taken into account by any workers.

Baffles in a bed greatly reduce the bed expansion and therefore increase the particle count in a photographed area. This is obvious from a comparison of photographs taken with a bed both with and without baffles. The great difference in the homogeneity between a free bed and a baffled bed is illustrated in Figures 1 and 2. Baffles reduce the spin of the particles and also their linear velocity.

Table 1 and a comparison of Figures 3 and 5 show the enormous effect of baffles on the particle motion. The average linear velocity in a baffled bed is reduced by a factor of about 5 to 1 or 10 to 1 as compared with a free bed. The frequency of peaks is greatly reduced and shows but little change as the gas flow rate is changed. A small difference exists between the choice of baffles *A* and *B*, as seen by a comparison of runs 2 and 7 or 1 and 6. The smaller mesh resulted in the smaller average velocity. Increasing the gas velocity caused an increase in the particle average velocity as shown by a comparison of runs 1 and 2 or 6 and 7. If the gas velocity is sufficiently low, a

TABLE 1. SUMMARY OF DATA FOR STUDY OF PATTERN OF FLOW OF SOLIDS

Run	Solids	Amount of solids, lb.	Settled bed hgt. L_o, ft.	Fluidized bed hgt., ft.	Superficial gas velocity lb./(hr.)(sq. ft.)	Superficial gas velocity ft./sec.	Baffle design	Location*, in.	Camera speed, frames/sec.	R.M.S. particle velocity, ft./sec.	Max. velocity of particles, ft./sec. Up	Max. velocity of particles, ft./sec. Down
1	Glass	5.40	0.80	0.98	635	2.2	*B*	1.97	960	0.27	0.72	0.70
2	Glass	5.91	0.88	0.98	450	1.55	*B*	1.97	1,200	0.17	0.96	0.99
3	Glass	3.66	0.54	0.98	1,225	4.2	*B*	1.97	1,920	0.22	0.81	0.72
4	Glass	3.66	0.51	Varied	1,225	4.2	None	1.97	1,820	2.44	7.15	6.39
5	Glass	5.40	0.75	Varied	635	2.2	None	1.97	1,800	1.96	2.23	5.70
6	Glass	5.40	0.80	0.98	635	2.2	*A*	1.97	1,920	0.43	0.97	1.55
7	Glass	5.91	0.88	0.98	450	1.55	*A*	1.97	1,080	0.22	0.97	0.99
11	Alumina	5.04	1.08	Varied	82	0.29	None	1.58	2,040	0.38	0.22	1.24
12	Alumina	5.04	1.08	Varied	114	0.39	None	1.58	1,920	0.75	0.75	2.30
13	Alumina	5.04	1.08	—	114	0.39	*C*	1.58	2,160	0.30	0.49	1.01

* Distance between the photographed field and the top of the fluidized bed.

portion of a fluidized bed can become stagnant temporarily. This is particularly likely in a baffled bed. During run 2 the photographed section of the bed showed no motion for about 30% of the time. Runs 1, 5, and 6 showed that baffles *A* produced more peak velocities upward than were observed with baffles *B* or with a free bed.

Alumina Particles

Table 1 shows data for three runs with alumina. One set is shown in Figure 6. Velocity peaks and flow reversals are similar to the effects noted for the larger glass particles. The effect of increasing gas flow is similar.

Although the values of G/G_o were higher for the alumina, the velocities of the alumina particles were less than those for the glass beads. The probable reason is the greater severity of slugging with the glass beads. Thus alumina particles moved at roughly one-fifth the velocity of the glass particles, for free-fluidized beds of equal bed expansions. The superficial gas velocity for the runs with alumina was 0.29 and 0.39 ft./sec. compared with 2.2 and 4.2 ft./sec. for the glass beads.

One difference between the alumina and the glass particles was that baffles reduced the average velocity of the alumina particles by about 3 to 1, a much smaller change than was noted with the glass beads.

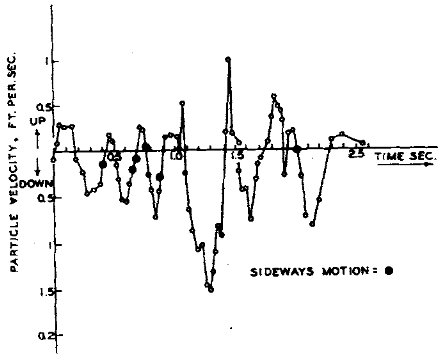

Fig. 5. Effect of baffles. Run 6, same as run 5 except that baffles *A* were installed.

Remarks on Temperature Profile

The solids flow pattern explain certain heat transfer observations. A prior study (*13*) made with a bed having the same diameter, height, baffle design, solids, gas, and gas velocities shows temperature measurements along the geometric axis. Air entered at about 90°C.; the walls were cooled with water at about 30°C. For free fluidization a near-constant temperature profile resulted for a gas flow which was 1.2 times the flow for incipient fluidization. For a baffled bed the profile was not this flat until the gas velocity was increased beyond the incipient value by over 100%. Thus although baffles prevent channeling and slugging, they cause some impoverishment in the heat exchange between one region in the bed and another. The reason of course is that baffles decrease the average velocity of the particles.

Particle Diffusivity

Runs 6 and 7 were duplicates of prior runs (*12*) carried out to determine diffusivities of the solid particles. In the early work trace particles were dropped on the top of a fluidized bed, and samples were removed at a point 4.7 in. below. Concentration vs. time data were used to calculate diffusivities for the particles. These prior tests were designed to test the equation of Trawinsky (*25*) which extended the kinetic molecular theory of Shafer:

$$D = (K/1 - \epsilon_o)\, G\, d\, (\Delta L/L_o) \quad (1)$$

The equation could not be checked for a free-fluidized bed, presumably because of nonuniformities in the gas-solid system, but the results were promising for baffled beds. A linear relationship was obtained for the prior data:

$$D = 0.050\, (G)\, (\Delta L/L_o) \quad (2)$$

The present photographs permit an independent check of the equation. A convenient comparison can be made in terms of the average velocity of the particles. For run 7 the relative expansion of the bed was 0.11, and the particle diffusivity was 2.5 sq. ft./hr. Einstein's expression $V = 2D/\Delta X$ and the expression $\Delta X = (\pi\sqrt{2}\, n\, d^2)^{-1}$ combine to give a corresponding velocity of about 3 ft./sec. for the particles. The motion picture evidence showed that the particle root-mean-square velocity at the walls was 0.22 ft./sec. A similar discrepancy exists for run 6; the diffusivity value from Equation (2) coupled with the bed expansion of 0.22 leads to a predicted velocity of about 6 ft./sec., whereas the photographs show an actual R.M.S. velocity of 0.43 ft./sec. The discrepancy of about 15 to 1 between the predicted velocities and the observed velocities can be explained. The equations assume that the kinetic molecular theory applies to individual solid particles and that each particle moves as an individual. The motion pictures show that aggregates of particles move as a unit, even in baffled beds. The particles in an aggregate have approximately the same velocity in the same direction. Perhaps one should use the average diameter of an aggregate and the number of aggregates per unit volume in the above equations instead of the particle diameter and concentration. At present these

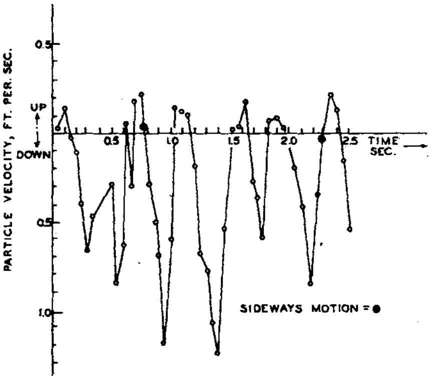

Fig. 6. Velocity of 200-mesh alumina powder at the wall. Run 11, no baffles, superficial air velocity = 0.29 ft./sec.

suggested measurements are not available.

It is significant that the diffusivity of the particles in the baffled bed is of rather small magnitude. This means that a well-baffled bed is more like a fixed bed than a free-fluidized bed, at least from the standpoint of the circulation of the solids.

GAS FLOW PATTERN

Previous investigators have been greatly concerned with the gas flow pattern in fluidized beds. The performance of fluidized reactors and the variables affecting the gas flow pattern have been referred to by numerous workers (*4 to 10, 17, 18, 24, 25, 29, 30*). The process of bubbling has received special attention. Baumgarten and Pigford (3) consider it from the standpoints of the extent of bubbling and the conditions under which it occurs. Rice and Wilhelm (*19*) consider the dynamics of the boundary between the dense suspension and the gas bypassing as bubbles. Other problems involve the amount of bypassing gas and the stability of the above-named boundary. The phase boundary may sometimes seem to be lacking or nonexistent in short columns; however it has been shown that a uniform distribution of solid particles is unstable, and if a column is of sufficient height, growing bubbles of gas must always appear (*1*).

It is important whether bubbles do or do not occur because bubbles affect the gas-solid mixing. Two counteracting effects take place when the gas velocity is increased. One has been pointed out by Toomey and Johnstone (*24*) and Trawinski (*25*), who show that the number of bubbles increases. Because bubbles represent bypassing gas, this effect should cause a reduction in the rates of heat and mass transfer. The second effect of velocity increase is an increase in the agitation of the particles in the phase boundaries. Of course this tends to cause improvement in the heat and mass transfer. Which effect predominates depends on the operating conditions, but the second effect seems to be more significant in most experiments. Shen and Johnstone (*20*) found that increases in the gas velocity caused increases in the heat and mass transfer between the solids and the gas. Massimilla and Johnstone (*14*) obtained similar results. Shuster and Kisliak (*21*) found that the bed uniformity increased up to a certain gas velocity. On the other hand Mathis and Watson (*16*) found that for the dealkylation of cumene the conversion depended on the flow rate in a complex fashion, with increases and decreases both being possible as the velocity increases.

Bubbling is analogous to the rise of gas bubbles in a liquid. Toomey and Johnstone (*24*) have suggested that a simple model for a fluidized bed is obtained by imagining bubbles of pure gas to rise through a second dense phase, a uniform suspension. Trawinski (*25*) stated that bubbles form at the bottom of a bed and begin to rise only when they are sufficiently large to overcome downward forces. The use of Stokes's law was suggested because the Reynolds numbers were small.

Runs 8, 9, and 10 were conducted to study bubbling in the absence of baffles. The conditions are summarized in Table 2. The remainder of this paper consists of observations based on the motion pictures for those runs.

For run 9 two patterns of gas flow occurred at 0.6 in. from the bottom. Type 1 consisted of cavities that passed through the field of view with no substantial modifications beyond certain deformations somewhat similar to those which occur also for gas bubbles in liquids. These bubbles can be classified according to size. The bigger bubbles of, say, 0.5-in. diameter moved rapidly upward (at about 1 ft./sec.). Very few solids were suspended in these bubbles. The boundary surfaces were not spherical but were well defined. Surrounding particles in the dense phase showed a pronounced motion downward as these bubbles rose. Very small cavities occur also. Figure 7 illustrates a bubble of about 0.06-in. diameter. Both the bubble and the surrounding phase moved upward with their absolute velocities being 0.70 and 0.57 ft./sec.

TABLE 2. SUMMARY OF DATA FOR STUDY OF PATTERN OF GAS FLOW
Solids: 120- to 200-Mesh Alumina

Run	Settled bed height L_o, ft.	Superficial gas velocity, lb./(hr.)(sq. ft.) Main feed	Injected	Location*, in.	Height of field of view, in.	Camera speed, frames/sec.	Notes
8	0.89	28.5	3.1	2.4	0.33	1,920	Injection nozzle of ¼-in. tubing.
9	0.89	31.6	0	0.6	0.33	2,160	Column inclined 10 deg.
10	1.08	31.6	0	6.9	3.5	2,160	Inclined 10 deg.

* Distance between the photographed field and the bottom of the fluidized bed.

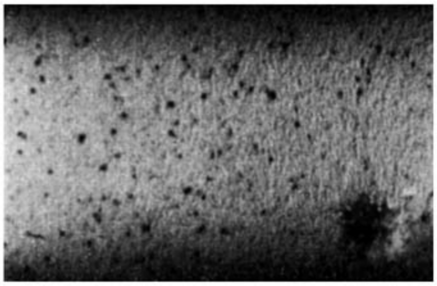

a

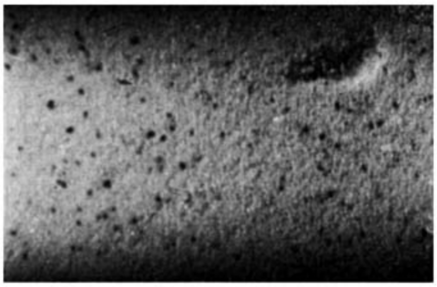

b

Fig. 7. Small bubble rising in alumina. Bubble width = about 0.06 in. Height of view = 0.33 in. Run 9 at 1,200 frames/sec., (*a*) frame 0, (*b*) frame 28.

The equations of Baron and Mugele (*1*) can be used to estimate the largest bubble which could be empty of solids for an appreciable time. The viscosity of the dense phase can be guessed as roughly 250 centipoise by comparing the solid to some described in the literature (*15*). This leads to a value of 0.94 in. for the maximum diameter of stable empty bubbles. The bubbles described above were smaller than this.

Some cavities originated, grew, decreased, and vanished in the small field of view (0.47 × 0.33 in.) during run 9; these are type 2, also called gas pockets herein. Typically the birth of such a cavity starts as a small hole which moves upward splitting the dense phase like a wedge. The cavity then expands, with a typical increase in width occurring at a rate of about 0.43 ft./sec. Eventually the growth ceases, and collapse sets in. Collapse frequently takes place by a break in the roof of the cavity which allows simultaneous leakage of solids inward and gas outward and a rise of solids from below. Occasionally the roof of a cavity breaks at one point only. Then the gas leaks out quickly, possibly to form a new cavity at a higher elevation.

Type 2 cavities should not be likened to bubbles in a liquid. Rather these cavities appear to be regions of high gas pressure. As the gas enters a zone having a minor resistance to gas flow, it blasts open a cavity. The cavity grows until a rupture occurs which provides a leak into a new zone or zones of minor resistance. Collapse occurs as the pressure falls. This gas motion is quite

Fig. 8. Collapsing gas pockets. 3.75-in. column, inclined 10 deg., run 13, 200-mesh alumina.

unlike that of gas bubbles in a liquid. The motion of type 2 cavities or pockets is slow compared with that of type 1 bubbles. The gas inside type 2 cavities does not possess enough energy to split the bed all the way up. Instead the gas inside is destined usually to leak into new zones to form new pockets. However two interesting possibilities exist and seem to occur; the gas can be partly captured by fast bubbles passing by or can simply leak in all directions and become distributed throughout the dense phase.

Photographs midway up the bed for run 10 showed gas flow patterns similar to those near the bottom. One exception was that formation of cavities by the coalescence of two or more bubbles was frequent in the midsection. Such cavities moved faster than cavities near the bottom. Figure 8 illustrates a typical large pocket near the midsection of the bed. A rain of particles down from the roof of the cavity occurs in the picture. The prominent cavities in these photographs are larger than the theoretical critical size of 0.94 in.

Run 8 included the injection of about 10% of the gas at a fixed point in the bed. Motion pictures showed discrete small bubbles at this point indicating that the gas injection was discontinuous. The same thing occurs of course when gas is injected into a liquid from an orifice. The motion of the surroundings, first outward, then down and in to pinch off the bubble, is quite evident when solids are present. The last part of this solids movement is much faster than the earlier part.

The gas flow patterns can be used to postulate why the difference between the conversion in a fluidized and in a fixed bed can first decrease and then increase as the flow rate is progressively increased. At low flow rates small bubbles and quasistable pockets predominate. These move rapidly through the bed with the gas inside excluded from good contact with the catalyst powder. At higher flow rates unstable pockets predominate. The rain of solids through these slow-moving pockets provides contact for catalysis, and the efficiency of the reactor is thus improved. Eventually a flow rate could be reached which would be so great that severe channeling would result and finally the bed would become inoperable. This extreme case was not studied in the present investigation. It was reached in tests on a catalytic reactor described by Mathis and Watson (*16*).

ACKNOWLEDGMENT

The authors express appreciation to the Italian Rotary Clubs for a fellowship for part of the work. Helpful advice in analyzing motion pictures was given by V. E. Putnam. The preparation of the manuscript was aided by Virgilio Causa.

NOTATION

d = average diameter of particles, ft.
D = diffusivity of solid particles, sq. ft./hr.
G = superficial gas flow rate, lb./(hr.) (sq. ft.)
G_o = superficial gas flow rate for incipient fluidization, lb./(hr.) (sq. ft.)
K = dimensional constant cu. ft./lb.
L_o = settled height of bed, ft.
ΔL = bed expansion, ft.
n = number of particles per unit volume, $ft.^{-3}$
V = particle velocity, ft./hr.
ΔX = particle displacement, ft.
ϵ_o = fractional voids in settled bed, dimensionless

LITERATURE CITED

1. Baron, Thomas, and R. A. Mugele, *A.I.Ch.E. Journal*, to be published.
2. Bart, Roger, D. Sc. thesis, Mass. Inst. Technol., Cambridge (1950).
3. Baumgarten, P. K., and R. L. Pigford, *A.I.Ch.E. Journal*, **6**, 1 (1960).
4. Brötz, Walter, *Chem.-Ing.-Tech.*, **24**, 60 (1952).
5. Gilliland, E. R., and E. A. Mason, *Ind. Eng. Chem.*, **41**, 1191 (1949).
6. *Ibid.*, **44**, 218 (1952).
7. ———, and R. C. Oliver, *ibid.*, **45**, 1177 (1953).
8. Leva, Max, Murray Weintraub, and Milton Grummer, *Chem. Eng. Progr.*, **45**, 563 (1949).
9. ———, and Milton Grummer, *ibid.*, **48**, 307 (1952).
10. Lewis, W. K., E. R. Gilliland, and W. C. Bauer, *Ind. Eng. Chem.*, **41**, 1104 (1949).
11. Massimilla, Leopoldo, and Sergio Bracale, *Ricerca Sci.*, **26**, 487 (1956).
12. *Ibid.*, **27**, 1509 (1957).
13. ———, and Antonio Cabella, *ibid*, **27**, 1853 (1957).
14. Massimilla, Leopoldo, and H. F. Johnstone, in preparation.
15. Matheson, G. L., W. A. Herbst, and P. H. Holt, *Ind. Eng. Chem.*, **41**, 1099 (1949)
16. Mathis, J. F., and E. C. Watson, *A.I.Ch.E. Journal*, **2**, 518 (1956).
17. Morse, R. D., *Ind. Eng. Chem.*, **42**, 117 (1949).
18. ———, and C. O. Ballou, *Chem. Eng. Progr.*, **47**, 199 (1951).
19. Rice, W. J., and R. H. Wilhelm, *A.I.Ch.E. Journal*, **4**, 4 (1958).
20. Shen, C. Y., and H. F. Johnstone, *ibid.*, **1**, 349 (1955).
21. Shuster, W. W., and Peter Kisliak, *Chem. Eng. Progr.*, **48**, 455 (1952).
22. Todd, D. B., R. H. Overcashier, and D. B. Olney, Motion Picture, "Fluidization Characteristics in a Two-Dimensional Fluid Bed," Shell Development Company, Emeryville, California (1957)
23. Toomey, R. D., and H. F. Johnstone, *Chem. Eng. Progr. Symposium Ser. No. 5*, **49**, 51 (1953). (1953).
24. ———, *Chem. Eng. Progr.*, **48**, 220 (1952).
25. Trawinski, H., *Chem.-Ing.-Tech.*, **25**, 229 (1953).
26. Wamsley, W. W., and L. N. Johanson, *Chem. Eng. Progr.*, **50**, 347 (1954).
27. Westwater, J. W., *ibid.*, **55**, No. 6, 49 (1959).
28. ———, and Leopoldo Massimilla, Motion Picture "Photographic Study of Solid-Gas Fluidization," Univ. Ill., Urbana (1958).
29. Wicke, E., and H. Trawinski, *Chem.-Ing.-Tech.*, **25**, 114 (1953).
30. Wilhelm, R. H., and Mooson Kwauk, *Chem. Eng. Progr.*, **44**, 201 (1948).

Manuscript received November 17, 1958; revision received August 3, 1959; paper accepted August 10, 1959. Paper presented at A.I.Ch.E. Cincinnati meeting.